Supplementary material

Reversible Hydrogen Storage in Yttrium Aluminum Hydride

Zhijie Cao[a,b,c], Liuzhang Ouyang[a,b,d]*, Hui Wang[a,b], Jiangwen Liu[a,b], Michael Felderhoff [c]*, Min Zhu[a,b]

[a]School of Materials Science and Engineering, Key Laboratory of Advanced Energy Storage Materials of Guangdong Province, South China University of Technology, Guangzhou, 510641, PR China

[b]China-Australia Joint Laboratory for Energy & Environmental Materials, South China University of Technology, Guangzhou, 510641, PR China

[c]Max-Planck-Institut für Kohlenforschung, Kaiser-Wilhelm-Platz 1, 45470 Mülheim, Germany

[d]Key Laboratory for Fuel Cell Technology in Guangdong Province, Guangzhou, 510641, PR China

*Corresponding author: Liuzhang Ouyang, E-mail: meouyang@scut.edu.cn; Fax: 86-20-87112762.
Michael Felderhoff, E-mail: felderhoff@mpi-muelheim.mpg.de. Tel.: 49(0)2083062368.

Experimental section

Commercial anhydrous YCl_3 (99.99 wt%) and $LiAlH_4$ (97 wt%) were used as the starting materials without further purification. A mixture of $LiAlH_4$ and anhydrous YCl_3 at a molar ratio of 3:1 (referred to as YCl_3−$3LiAlH_4$) was ball milled for 6 h on a QM−3SP4 planetary ball mill rotating at a speed of 500 rpm. The ball-to-powder weight ratio was chosen as 40:1. To suppress the possible decomposition of the product, the milling process was conducted under a hydrogen pressure of 8 MPa. Besides, the milling procedure was set as alternating 30 min of milling and 30 min of rest to avoid the increase of temperature inside the jar. Before milling, all sample handlings were performed in a glovebox with a moisture content of less than 3 ppm and an oxygen content of less than 5 ppm.

The microstructures of samples were characterized using X-ray diffraction analysis (XRD, Rigaku MiniFlex 600) with Cu-K_α radiation (λ = 0.15406 nm). To avoid any oxidation during the measurement process, the XRD samples were first loaded into a homemade sealed sample stage in the glovebox. Before these measurements, a high purity (99.9999 %) silicon wafer was used to calibrate the instrumental zero-shift. The hydrogen storage properties and temperature programmed-desorption (TPD) for volumetric quantitative measurements were evaluated through a Sieverts-type automatic gas reaction controller (Advanced Materials Corporation). For each measurement, 0.1 g of powder was placed into the sample cell, which was inductively heated with an accuracy of ±2 °C. Hydrogen release was also detected using mass spectrometry (MS, Hiden, Qic20) over a temperature range from 40 to 400 °C at a heating rate of 4 °C/min with an argon purge rate of 30 mL min^{-1}. The chemical bonding states were identified using Fouriertransform infrared spectroscopy (FT−IR, Nicolet IS50). The samples were pressed with anhydrous potassium bromide (KBr) powder. Differetial scanning calorimetry (DSC) was performed on a Setaram Sensys Evo Instrumentation at a heating rate of 4 ^oC/min.

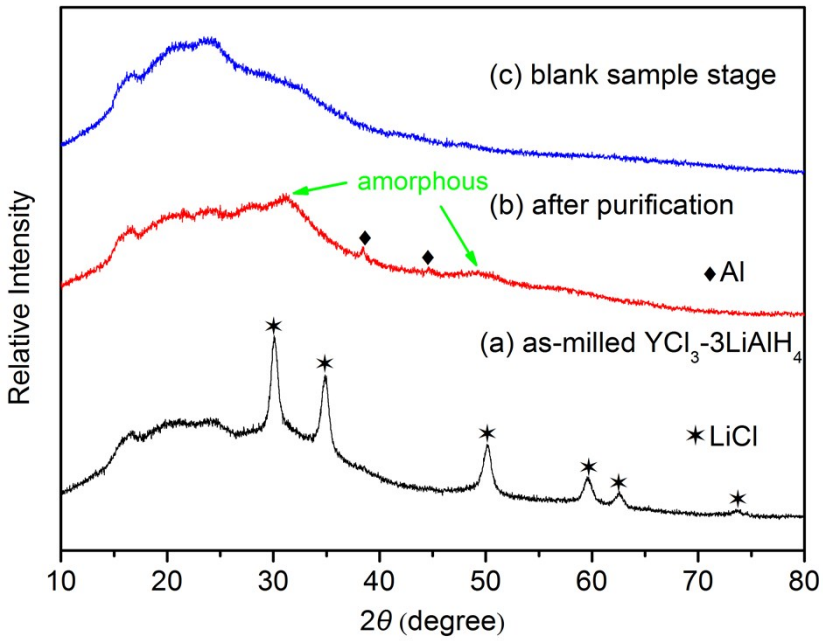

Fig. S1 XRD patterns of (a) as-milled YCl_3-3$LiAlH_4$, (b) sample after the removement of LiCl via an extraction with diethylether and drying procedure, (c) blank sample stage.

The as-milled YCl_3-3$LiAlH_4$ was purified via an extraction with diethylether and drying procedure to remove LiCl from the product. As shown Figure S1b (red line), two broad peaks show up after the removement of LiCl, which indicates the amorphous structure of $Y(AlH_4)_3$.

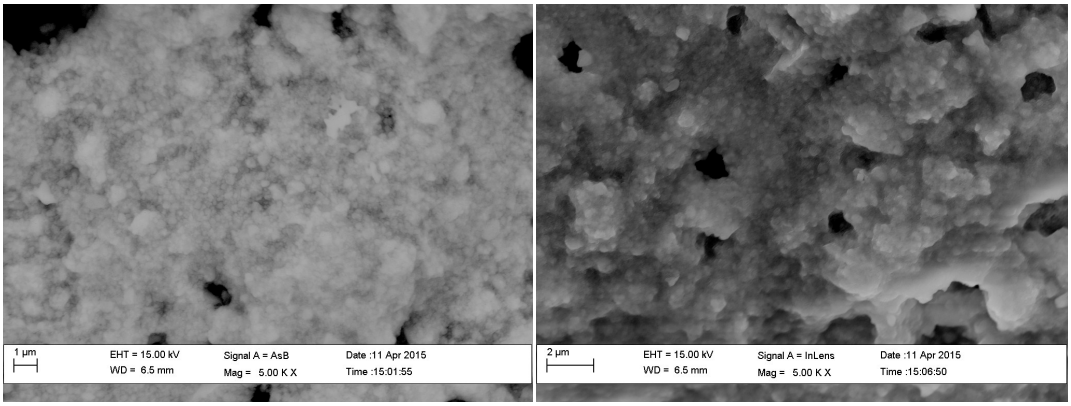

Fig. S2 SEM of as-milled $Y(AlH_4)_3$-3LiCl.

As shown in Figure S2, $Y(AlH_4)_3$ is extremely sensitive to moisture and atmospheric oxygen, and any contact with air would result in its vigorous hydrolysis with the evolution of hydrogen, which resulted in the formation of pores in the sample.

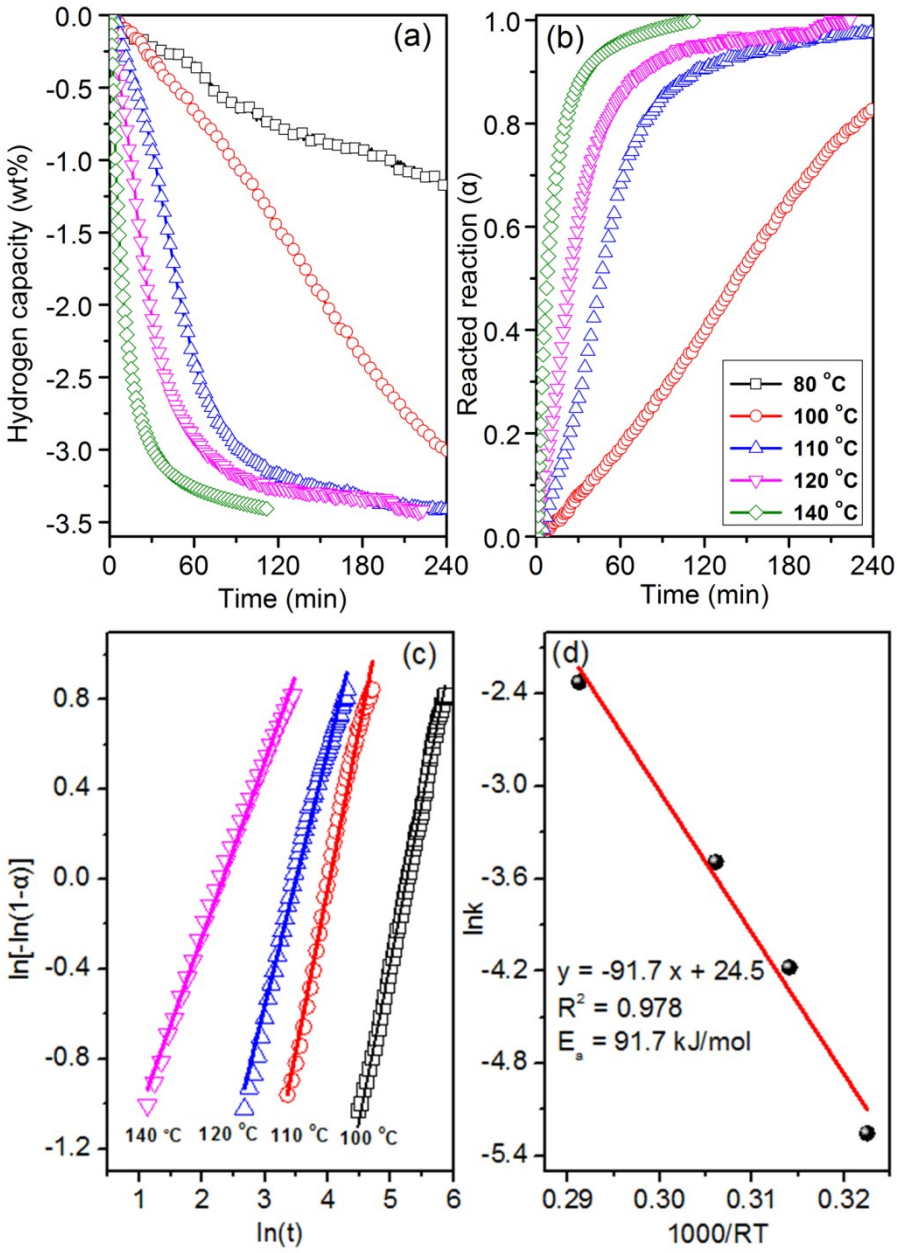

Fig. S3 (a) Isothermal dehydrogenation curves and (b) Isothermal dehydrogenation rate curves at different temperature. The wt% H_2 values are normalized to the $Y(AlH_4)_3$ percentage.
(c) Plot of ln[−ln(1−α)] vs. ln t fitted by the JMAK equation and (d) Arrhenius plots.

As shown in Figure S3a, $Y(AlH_4)_3$ can release ~1.2 wt% H_2 within 240 min even at a low temperature of 80 °C. The hydrogen desorption speeds up dramatically with increasing temperature. At 110 °C, ~3.4 wt% H_2 can be released within 200 min, while it only takes ~60 min to liberate the same amount of hydrogen at 140 °C. As shown in Figure S3b, ninety percent of the hydrogen can be released within 103 min at 110 °C, and this value decreases to ~30 min when increasing temperature to 140 °C. To further understand the first dehydrogenation step of $Y(AlH_4)_3$, the

isothermal desorption kinetics curves were analyzed with the Johanson–Mehl–Avrami–Kolmogorov (JMAK) equation: [S1]

$$[-\ln(1-\alpha)]^{1/\eta} = kt$$

where α is the reaction fraction, k is the rate constant, and η is the Avrami exponent. The JMAK equation is based on nucleation and growth events, and is widely used to describe the time-dependent kinetic behavior of isothermal solid-state reactions.[S2] As shown in S3c, ln[−ln(1−α)] varied linearly with ln t over the range from 0.2 to 0.9, with a linearity constant of $R^2 > 0.99$, indicating that the JMAK equation could indeed be used to describe the first-step dehydrogenation process. The temperature dependence k obtained above can be applied to calculate the dehydrogenation activation energy using the Arrhenius equation. As shown in Figure S3d, the activation energy for the dehydrogenation of $Y(AlH_4)_3$ was estimated be 91.7 kJ mol^{-1}, which was much smaller than that of nanocrystalline rod $Mg(AlH_4)_2$ (123.0 kJ mol^{-1}).[S3]

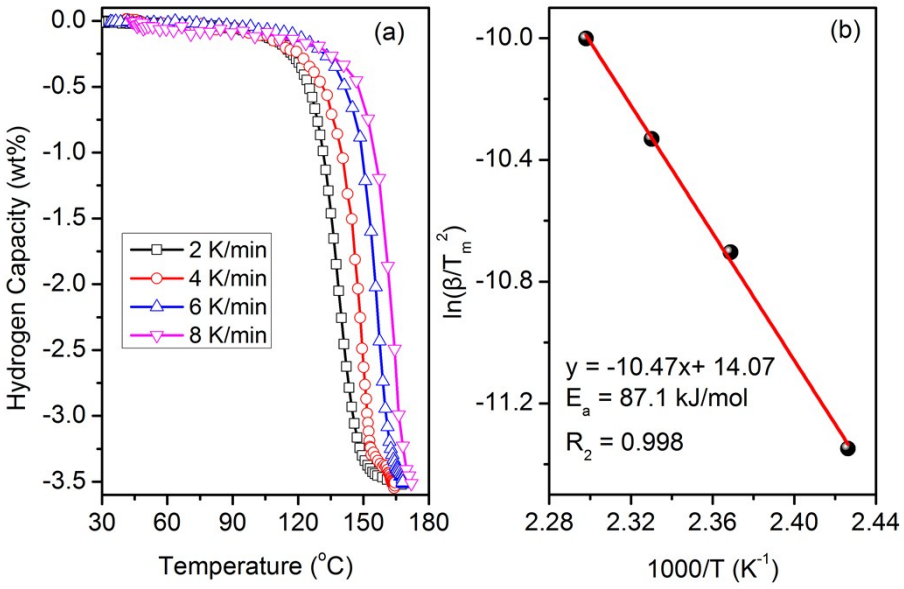

Fig. S4 (a) Dehydrogenation curves at variable heating rates and (b) Kissinger plot of $Y(AlH_4)_3$ The wt% H_2 values are normalized to the $Y(AlH_4)_3$ percentage.

The kinetic barrier of the first-step dehydrogenation was also confirmed by using the Kissinger method:[S4-6]

$$\ln\left(\frac{\beta}{T_m^2}\right) = -\frac{E_a}{RT_m} + C$$

Where β is the heating rate, T_m is the absolute temperature for the maximum reaction rate, R is the gas constant and C is a constant. Figure S4a shows the TPD curves at variable heating rates (2-8

k/min) of $Y(AlH_4)_3$. The temperatures (T_m) were extracted from the maximum reaction rate. Figure S4b reveals the Kissinger plot of the first dehydrogenation step. The apparent dehydrogenation activation energy was calculated to be ~87.1 kJ mol^{-1}, which was consistent with the value of 91.7 kJ mol^{-1} above.

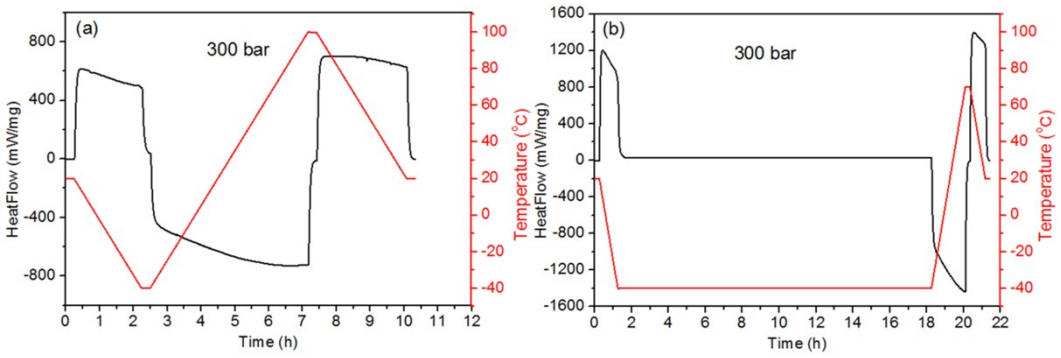

Fig. S5. High-pressure DSC curves of YAl_3 under 300 bar at (a) -40 °C~100 °C and (b) -40 °C.

Rehydrogenation of $RE(AlH_4)_3$ were impossible when they decomposed into the final product $REAl_3$.[S7] Also Al_3Mg_2 alloy could not be rehydrogenated back to $Mg(AlH_4)_2$ under 100 bar of hydrogen pressure at temperatures ranging from 25 to 210 °C.[S3] Through high pressure DSC measurement, as shown in Figure S5. The YAl_3 alloy can not be hydrogenated back to hydrides at -40 °C~100 °C even under a high pressure of 300 bar. Hence in this work, it was reasonably proposed that $Y(AlH_4)_3$ can not be rehydrogenated back once it decomposed into YAl_3. These compounds are only possibly reversible under extremely harsh conditions, i.e., extremely low temperature and/or extremely high pressure.

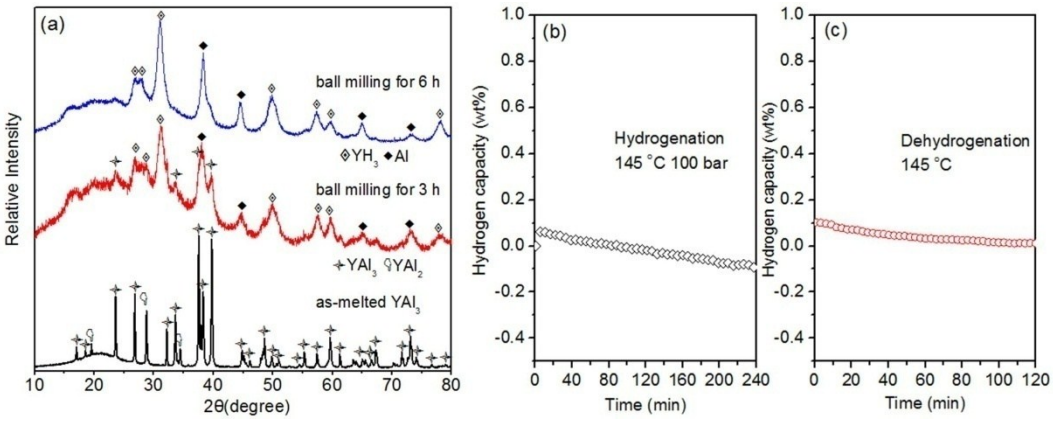

Figure S6. (a) XRD patterns of YAl_3 after ball milling for different time under 80 bar, (b) isothermal absorption under 100 bar H_2 at 145 °C of *in-suit* composite of YH_3 and Al and (c) the corresponding desorption kinetic curves.

YAl_3 alloy was ball milled under a hydrogen pressure of 80 bar. As shown in Figure S6a, YAl_3 alloy completely decomposed into YH_3 and Al after ball milling for 6 h. Then this *in-suit* composite of YH_3 and Al was subjected to hydrogenation under 100 bar H_2 at 145 °C. As shown in Figure S6b and c, not any hydrogen absorption and desorption can be observed in this *in-suit* composite.

References

S1 M. Avrami, *J. Chem. Phys.*, 1939, 7, 1103–1112.

S2 K. F. Kelton, *Mater. Sci. Eng, A*, 1997, **226–228**, 142-150.

S3 Y. Liu, Y. Pang, X. Zhang, Y. Zhou, M. Gao and H. Pan, *Int. J. Hydrogen Energy*, 2012, **37**, 18148–18154.

S4 J. Augis and J. Bennett, *J. Therm. Anal. Calorim.*, 1978, **13**, 28–3292.

S5 C. Zlotea, M. Sahlberg, S. Özbilen, P. Moretto and Y. Andersson, *Acta. Mater.*, 2008, **56**, 2421–2428.

S6 X. B. Yu, Y. H. Guo, D. L. Sun, Z. X. Yang, A. Ranjbar, Z. P. Guo, H. K. Liu and S. X. Dou, *J. Phys. Chem. C*, 2010, **114**, 473–34737.

S7 C. Weidenthaler, A. Pommerin, M. Felderhoff, W. Sun, C. Wolverton, B. Bogdanović and F. Schüth, *J. Am. Chem. Soc.*, 2009, **131**, 16735–16743.